Colloidal Graphite-Assisted Laser Desorption/Ionization MS and MS n of Small Molecules. 2. Direct Profiling and MS Imaging of Small Metabolites from Fruits

ARTICLE *in* ANALYTICAL CHEMISTRY · SEPTEMBER 2007

Impact Factor: 5.64 · DOI: 10.1021/ac0706170 · Source: PubMed

3 AUTHORS, INCLUDING:

Sangwon Cha
Hankuk University of Foreign Studies
21 PUBLICATIONS **477** CITATIONS

SEE PROFILE

Anal. Chem. **2007,** *79,* 6575−6584

Colloidal Graphite-Assisted Laser Desorption/Ionization MS and MS^n of Small Molecules. 2. Direct Profiling and MS Imaging of Small Metabolites from Fruits

Hui Zhang, Sangwon Cha, and Edward S. Yeung*

Ames Laboratory—USDOE and Department of Chemistry, Iowa State University, Ames, Iowa 50011

Due to a high background in the low-mass region, conventional MALDI is not as useful for detecting small molecules (molecular masses <500 Da) as it is for large ones. Also, spatial inhomogeneity that is inherent to crystalline matrixes can degrade resolution in imaging mass spectrometry (IMS). In this study, colloidal graphite was investigated as an alternative matrix for laser desorption/ionization (GALDI) in IMS. We demonstrate its advantages over conventional MALDI in the detection of small molecules such as organic acids, flavonoids, and oligosaccharides. GALDI provides good sensitivity for such small molecules. The detection limit of fatty acids and flavonoids in the negative-ion mode are in the low-femtomole range. Molecules were detected directly and identified by comparing the MS and MS/MS spectra with those of standards. Various fruits were chosen to evaluate the practical utility of GALDI since many types of small molecules are present in them. Distribution of these small molecules in the fruit was investigated by using IMS and IMS/MS.

Matrix-assisted laser desorption/ionization mass spectrometry (MALDI MS) has been extensively used for the analysis of large molecules such as proteins[1] and synthetic polymers.[2] The key features of MALDI MS are its soft ionization characteristic and simplified spectra as mostly singly charged species are generated. Compared to electrospray ionization (ESI) MS, MALDI bears other advantages such as better tolerance to interference from salts and buffers and simpler sample preparation. MALDI has also proven to be very useful for the analysis of medium-size molecules (500−10 kDa) such as peptides,[3] oligonucleotides,[4] and oligosaccharides.[5] However, the analysis of small molecules (<500 Da) by conventional MALDI MS is far less successful than that of larger molecules because the analyte ions are strongly interfered with or are suppressed by the matrix-related ions that are predominant at the low m/z range.

Different approaches have been employed in MALDI MS to minimize the background in the low-mass range. Reports includes derivatization of the analyte molecules to a higher molecular weight[6] or using a matrix with higher molecular weight such as porphyrin (MW 974.6).[7] Extra sample preparation was then needed, thereby limiting the classes of analytes that can be detected. It has been observed that matrix ions can be suppressed dramatically, and sometimes complete suppression can be achieved under well-controlled conditions.[8,9] For example, surfactant additives such as cetyltrimethylammonium bromide have been reported to substantially suppress the background from α-cyano-4-hydroxycinnamic acid (CHCA).[10] Laser intensity and the relative molar ratio of matrix to analyte are the major parameters to adjust. However, a suitable molar ratio is not always achievable especially for native biological samples.

Many inorganic materials have been tested as matrixes for surface-assisted laser desorption/ionization (SALDI), including different metal powders and metal oxide nanoparticles such as Ag, Au, Co, Al, Mn, Mo, Zn, Sn, W, Fe_3O_4, SnO_2, TiO_2, WO_3, ZnO, etc.[11−15] Generally, those SALDI MS can provide a cleaner background than conventional MALDI MS as no interference peaks from fragment ions of the organic matrixes were present. Another matrix-free approach for laser desorption/ionization on porous silicon was extensively studied since 1999.[16,17] Porous

* Corresponding author. E-mail: yeung@ameslab.gov.

(1) Karas, M.; Hillenkamp, F. *Anal. Chem.* **1988**, *60*, 2299−2301.
(2) Bahr, U.; Deppe, A.; Karas, M.; Hillenkamp, F.; Giessmann, U. *Anal. Chem.* **1992**, *64*, 2866−2869.
(3) Kaufmann, R.; Kirsch, D.; Spengler, B. *Int. J. Mass Spectrom. Ion Processes* **1994**, *131*, 355−385.
(4) Lecchi, P.; Pannell, L. K. *J. Am. Soc. Mass Spectrom.* **1995**, *6*, 972−975.
(5) Finke, B.; Stahl, B.; Pfenninger, A.; Karas, M.; Daniel, H.; Sawatzki, G. *Anal. Chem.* **1999**, *71*, 3755−3762.
(6) Tholey, A.; Wittmann, C.; Kang, M. J.; Bungert, D.; Hollemeyer, K.; Heinzle, E. *J. Mass Spectrom.* **2002**, *37*, 963−973.
(7) Ayorinde, F. O.; Hambright, P.; Porter, T. N.; Keith, Q. L. *Rapid Commun. Mass Spectrom.* **1999**, *13*, 2474−2479.
(8) Knochenmuss, R.; Dubois, F.; Dale, M. J.; Zenobi, R. *Rapid Commun. Mass Spectrom.* **1996**, *10*, 871−877.
(9) Knochenmuss, R.; Karbach, V.; Wiesli, U.; Breuker, K.; Zenobi, R. *Rapid Commun. Mass Spectrom.* **1998**, *12*, 529−534.
(10) Guo, Z.; Zhang, Q. C.; Zou, H. F.; Guo, B. C.; Ni, J. Y. *Anal. Chem.* **2002**, *74*, 1637−1641.
(11) Sluszny, C.; Yeung, E. S.; Nikolau, B. J. *J. Am. Soc. Mass Spectrom.* **2005**, *16*, 107−115.
(12) Tanaka, K.; Waki, H.; Ido, Y.; Akita, S.; Yoshida, Y.; Yoshida, T.; Matsuo, T. *Rapid Commun. Mass Spectrom.* **1988**, *2*, 151−153.
(13) McLean, J. A.; Stumpo, K. A.; Russell, D. H. *J, Am. Chem. Soc.* **2005**, *127*, 5304−5305.
(14) Kinumi, T.; Saisu, T.; Takayama, M.; Niwa, H. *J. Mass Spectrom.* **2000**, *35*, 417−422.
(15) Chen, C. T.; Chen, Y. C. *Anal. Chem.* **2005**, *77*, 5912−5919.
(16) Wei, J.; Buriak, J. M.; Siuzdak, G. *Nature* **1999**, *399*, 243−246.

10.1021/ac0706170 CCC: $37.00
Published on Web 08/01/2007

silicon surfaces were etched from crystalline silicon chips with hydrofluoric acid and functionalized as the laser desorption/ionization matrix as well as trapping agents for analyte molecules. Small molecules including pharmaceuticals, nucleic acids, carbohydrates, and steroids were successfully detected.[18−20] In a more recent work, commercially available silicon nanoparticles were utilized as an LDI matrix and the silicon powder preparation was optimized for the analysis of small molecules.[21] Different kinds of carbon materials, including graphite particles,[22] graphite plates,[23,24] graphite suspension in different solvents,[25−27] graphite trapped in silicone polymer,[28] activated carbon powders,[29] functionalized carbon nanotubes[30−33] and fullerenes,[34] and more recently pencil lead,[35−37] have been suggested as alternative matrixes for LDI MS. Many kinds of analyte molecules over a wide mass range (100−6000 Da) have been detected, such as peptides,[26−29,32−36] phospholipids,[25] oligosaccharides,[30−33,35] fatty acids,[24,36] synthetic polymers,[23,26,31,35,37] and other various organic compounds.[22−37] A more detailed description of graphite−LDI can be found in our previous paper.[38] Recent reviews about small-molecule MALDI MS[39] and matrix-free LDI MS can be found elsewhere.[40]

Imaging mass spectrometry (IMS) has proven to be a powerful technology for direct profiling and imaging of elements and biomolecules in tissue sections. Secondary ion mass spectrometry (SIMS),[41,42] MALDI,[43−47] and direct electrospray ionization (DESI)[48] have been applied as desorption/ionization techniques for the IMS of molecules such as metal elements, peptides, proteins, lipids, and other metabolites. SIMS has the best spatial resolution among the three, and DESI requires the least sample preparation and allows true in situ measurement with the simplest instrumentation.[48] The spatial resolution of MALDI IMS is in between SIMS and DESI IMS, usually ranging from 80 to 200 μm in diameter. The diverse choices of lasers and matrixes make MALDI MS suitable for fast, simultaneous, and high-throughput analyses of metabolites from tissue samples. MALDI equipped with a UV laser has been successfully demonstrated for the imaging of peptides, proteins, and lipids.[43−47] Due to the high background problem as discussed earlier, there is limited application of UV-MALDI for imaging of small molecules (<500 Da). Infrared (IR) MALDI was introduced recently as a technique for imaging small metabolites from fruit samples.[49] Water is used as the natural matrix for IR MALDI, but it is inevitable that the sample may dry out during the process of IR irradiation. Different locations will thus give different sensitivities due to inhomogeneous water content. So far, molecules that can be detected by IR MALDI are quite limited, either because of the low desorption/ionization efficiency or low detection sensitivity. Furthermore, the spatial resolution of IR-IMS is inherently worse than that of UV-IMS.

Previously we demonstrated that colloidal graphite was a good LDI matrix for the analysis of molecules in 500−1000 Da range, such as different lipid species.[38] This matrix contains fine particles and is spatially homogeneous, making it suitable for quantitative imaging. The colloidal property also allows it to be easily sprayed to form a layer on top of tissue samples and thus simplifies imaging experiments. In this study, we investigated the applicability of colloidal graphite as an alternative LDI matrix for the analysis of even smaller metabolite molecules. Fruits contain many kinds of small molecules such as long-chain fatty acids, small oligosaccharides, and flavonoids, so they serve as good systems to test the performance. GALDI MS and tandem MS were used to identify the ionized species, while IMS and IMS/MS were utilized to map the distribution of those molecules in fruit slices.

EXPERIMENTAL SECTION

Standards such as long-chain fatty acids, oligosaccharides, and flavonoids were purchased from Sigma-Aldrich (St. Louis, MO). Dihydroxybenzoic acid (DHB) from Bruker Daltonics (Billerica, MA) and CHCA solution from Agilent Technologies (Palo Alto, CA) were used as standard MALDI matrixes. 2-Propanol-based colloidal graphite aerosol spray (Aerodag G) was obtained from Acheson Colloids (Port Huron, MI). Pure water was obtained from a MilliQ water purification system (Billerica, MA). All other chemicals were purchased from Fisher Scientific (Fairlawn, NJ).

Apple and strawberry fruits were purchased from a local grocery store. Apple skin was peeled off by a sharp razor blade

(17) Shen, Z. X.; Thomas, J. J.; Averbuj, C.; Broo, K. M.; Engelhard, M.; Crowell, J. E.; Finn, M. G.; Siuzdak, G. *Anal. Chem.* **2001**, *73*, 612−619.
(18) Pihlainen, K.; Grigoras, K.; Franssila, S.; Ketola, R.; Kotiaho, T.; Kostiainen, R. *J. Mass Spectrom.* **2005**, *40*, 539−545.
(19) Compton, B. J.; Siuzdak, G. *Spectrosc.−Int. J.* **2003**, *17*, 699−713.
(20) Li, Q.; Ricardo, A.; Benner, S. A.; Winefordner, J. D.; Powell, D. H. *Anal. Chem.* **2005**, *77*, 4503−4508.
(21) Wen, X. J.; Dagan, S.; Wysocki, V. H. *Anal. Chem.* **2007**, *79*, 434−444.
(22) Zumbuhl, S.; Knochenmuss, R.; Wulfert, S.; Dubois, F.; Dale, M. J.; Zenobi, R. *Anal. Chem.* **1998**, *70*, 707−715.
(23) Kim, H. J.; Lee, J. K.; Park, S. J.; Ro, H. W.; Yoo, D. Y.; Yoon, D. Y. *Anal. Chem.* **2000**, *72*, 5673−5678.
(24) Park, K. H.; Kim, H. J. *Rapid Commun. Mass Spectrom.* **2001**, *15*, 1494−1499.
(25) Peng, S.; Edler, M.; Ahlmann, N.; Hoffmann, T.; Franzke, J. *Rapid Commun. Mass Spectrom.* **2005**, *19*, 2789−2793.
(26) Dale, M. J.; Knochenmuss, R.; Zenobi, R. *Anal. Chem.* **1996**, *68*, 3321−3329.
(27) Sunner, J.; Dratz, E.; Chen, Y. C. *Anal. Chem.* **1995**, *67*, 4335−4342.
(28) Li, X. P.; Wilm, M.; Franz, T. *Proteomics* **2005**, *5*, 1460−1471.
(29) Chen, Y. C.; Shiea, J.; Sunner, J. *J. Chromatogr.*, A **1998**, *826*, 77−86.
(30) Pan, C. S.; Xu, S. Y.; Hu, L. G.; Su, X. Y.; Ou, J. J.; Zou, H. F.; Guo, Z.; Zhang, Y.; Guo, B. C. *J. Am. Soc. Mass Spectrom.* **2005**, *16*, 883−892.
(31) Ren, S. F.; Zhang, L.; Cheng, Z. H.; Guo, Y. L. *J. Am. Soc. Mass Spectrom.* **2005**, *16*, 333−339.
(32) Ren, S. F.; Guo, Y. L. *Rapid Commun. Mass Spectrom.* **2005**, *19*, 255−260.
(33) Xu, S. Y.; Li, Y. F.; Zou, H. F.; Qiu, J. S.; Guo, Z.; Guo, B. C. *Anal. Chem.* **2003**, *75*, 6191−6195.
(34) Ugarov, M. V.; Egan, T.; Khabashesku, D. V.; Schultz, J. A.; Peng, H. Q.; Khabashesku, V. N.; Furutani, H.; Prather, K. S.; Wang, H. W. J.; Jackson, S. N.; Woods, A. S. *Anal. Chem.* **2004**, *76*, 6734−6742.
(35) Black, C.; Poile, C.; Langley, J.; Herniman, J. *Rapid Commun. Mass Spectrom.* **2006**, *20*, 1053−1060.
(36) Langley, G. J.; Herniman, J. M.; Townell, M. S. *Rapid Commun. Mass Spectrom.* **2007**, *21*, 180−190.
(37) Berger-Nicoletti, E.; Wurm, F.; Kilbinger, A. F. M.; Frey, H. *Macromolecules* **2007**, *40*, 746−751.
(38) Cha, S.; Yeung, E. S. *Anal. Chem.* **2007**, *79*, 2373−2385.
(39) Cohen, L. H.; Gusev, A. I. *Anal. Bioanal. Chem.* **2002**, *373*, 571−586.
(40) Peterson, D. S. *Mass Spectrom. Rev.* **2007**, *26*, 19−34.
(41) Altelaar, A. F. M.; Klinkert, I.; Jalink, K.; de Lange, R. P. J.; Adan, R. A. H.; Heeren, R. M. A.; Piersma, S. R. *Anal. Chem.* **2006**, *78*, 734−742.
(42) Ostrowski, S. G.; Van, Bell, C. T.; Winograd, N.; Ewing, A. G. *Science* **2004**, *305*, 71−73.
(43) Caprioli, R. M.; Farmer, T. B.; Gile, J. *Anal. Chem.* **1997**, *69*, 4751−4760.
(44) Chaurand, P.; Caprioli, R. M. *Electrophoresis* **2002**, *23*, 3125−3135.
(45) Chaurand, P.; Cornett, D. S.; Caprioli, R. M. *Curr. Opin. Biotechnol.* **2006**, *17*, 431−436.
(46) Garrett, T. J.; Prieto-Conaway, M. C.; Kovtoun, V.; Bui, H.; Izgarian, N.; Stafford, G.; Yost, R. A. *Int. J. Mass Spectrom. Ion Processes* **2007**, *260*, 166−176.
(47) Garrett, T. J.; Yost, R. A. *Anal. Chem.* **2006**, *78*, 2465−2469.
(48) Wiseman, J. M.; Ifa, D. R.; Song, Q. Y.; Cooks, R. G. *Angew. Chem., Int. Ed.* **2006**, *45*, 7188−7192.
(49) Li, Y.; Shrestha, B.; Vertes, A. *Anal. Chem.* **2007**, *79*, 523−532.

and attached to the stainless steel plate by double-sided tape. Apple juice was collected from crushed flesh onto a glass slide, dried and used directly. A cryostat from International Equipment Co. (Needham Heights, MA) was used for cryosectioning. Fruit chunks were dipped in liquid N_2 before they were cryosectioned into ~15-μm-thick specimens and stored at −20 °C before mass spectrometric analysis. No optimum cutting temperature (OCT) compounds were used to embed the fruit samples as the interference to mass spectra from OCT compounds is known.[50] Sectioned fruit slices were directly transferred and mounted onto the stainless steel plate. Before applying colloidal graphite solution, the slices were dried under moderate vacuum (~50 Torr) at room temperature for half an hour.

Long-chain fatty acid standards were prepared by dissolving stearic acid (C18, MW 284.48), pentacosanoic acid (C25, MW 382.66), hexacosanoic acid (C26, MW 396.69), octacosanoic acid-(C28, MW 424.74), and melissic acid (C30, MW 452.80) in chloroform to a final concentration of 200 pmol/μL each. For flavonoid standards, quercetin (MW 302.24), kaempferol (MW 286.23), phloretin (MW 274.27), and apigenin (MW 270.24) were dissolved individually in DMSO to give concentrations of 5 mg/mL each; then the four standard solution were mixed and further diluted to a final concentration of 200 pmol/μL each in water/acetonitrile/trifluoroacetic acid (49.95/49.95/0.1). Oligosaccharide standards were prepared by dissolving ribose (MW 150.13), glucose (MW 180.16), sucrose (MW 342.30), *N*-acetyl-D-lactosamine (LacNAc; MW 383.35), maltotriose (MW 504.44), and maltotetraose (MW 666.58) in water/acetonitrile/trifluoroacetic acid (49.95/49.95/0.1) to a final concentration of 100 ng/μL each. A 20 mg/mL DHB solution in 70% methanol and 30% water (containing a 0.1% trifluoroacetic acid) was prepared. Commercial Agilent CHCA solution at 6 mg/mL in 36/56/8 methanol/acetonitrile/water was purchased and used directly. Four times dilution of colloidal graphite solution with 2-propanol was used for GALDI MS and IMS.

For all mass spectrometric analyses and IMS, an LTQ linear ion trap mass spectrometer equipped with vMALDI source (Thermo Electron, Mountain View, CA) was used. The N_2 laser (337 nm) is guided to the source by a fiber-optic cable and has a maximum output of 280 μJ/pulse (before entering the optical fiber cable). The measured laser spot size is ~100 μm in diameter on the sample plate surface. A more detailed description of the LTQ with vMALDI source has been reported elsewhere.[46]

For conventional MALDI MS, 1 μL of DHB or CHCA matrix solution was applied onto the stainless steel sample plate and let dry in air, followed by 1 μL of sample solution on top of the matrix crystals. For GALDI MS of standards, 0.5 μL of diluted colloidal graphite solution was applied onto the stainless steel sample plate by a micropipet and let dry in air. Then 1 μL of standard solution was applied on top of the graphite spot. To obtain mass spectra from apple juice with GALDI, 1 μL of fresh apple juice was applied onto a dried (0.5 μL) graphite spot. For apple peels and fruit slices, diluted colloidal graphite solution was applied by a double-action airbrush (Aztek A470 with a 0.30-mm nozzle from Testor, Rockford, IL). The whole fruit slice was covered with colloidal graphite homogeneously by spraying with 20 psi air pressure and 15 cm away from the sample plate for 30 s. Peak identification was made by comparing both mass and tandem mass spectra with those of standards.

Optical images of fruit slices were taken inside the vMALDI source before IMS. Serial optical images were taken every 1-mm movement of the sample stage in either the *x*- or *y*-direction. Each segment of the images has a size of 140 pixels by 170 pixels. These segments of optical images were reconstructed as one optical image for one fruit slice. To collect mass spectra, the same sample plate was rastered with 100-μm steps. For each raster point, a mass spectrum was recorded for desorbed ions and integrated over three to five laser shots. In the cases of IMS/MS, target precursor ions (m/z 191 or 301) were first selected based on the mass spectral profiles of strawberry. Then the first-generation product ion spectra of the selected precursor ion were collected from all rastering points on the strawberry slice. More laser shots were required for MS^2 experiments and so nine laser shots were averaged for each raster point.

Custom software vMALDI data browser (Version 1.0) was used to extract mass spectra from specific locations and generate chemically selective images. This software was provided by the instrument vendor (Thermo Electron). The mass window for generating images was 0.5 Da. Intensities of the selected ion were normalized by dividing the total ion current of each mass spectrum. Then, chemically selective images were plotted as 3-D maps with the third dimension being the normalized intensity.

RESULTS AND DISCUSSION

MALDI and GALDI MS of Standard Mixtures of Fatty Acids, Flavonoids, and Oligosaccharides. Different classes of compounds were selected to compare the performance of conventional MALDI and GALDI. Long-chain fatty acids (C18−C30) were selected as one group of standards because of their important roles in many metabolic pathways of living organisms.[51] Fatty acids can be detected by GC/MS with proper derivatization such as esteritication to reduce the polarity and increase volatility.[52] HPLC−ESI MS can detect native fatty acids in the negative-ion mode through deprotonization.[53] However, the basic pH condition that is required to produce such negative ions is not compatible with most reversed-phase C18 columns that typically require acidic mobile phases. To overcome this problem, judicious derivatization was needed.[54] MALDI MS can eliminate the separation step but conventional MALDI matrixes do not work well for detection due to a high background and ion suppression in that mass region. This is underscored by the fact that none of the selected standard fatty acids were detected with DHB or CHCA in either positive-ion mode or negative-ion mode (data not shown). With GALDI, all five fatty acids (100 ng each) were detected as deprotonated peaks ($[M - H]^-$), as shown in Figure 1. It is noteworthy that the background in the negative-ion mode of GALDI is very clean up to at least m/z 1000 without any pretreatment. In fact, there are only a few low-number carbon cluster ions, such as $C12^-$−$C14^-$; and the intensity of such peaks is much lower than those for the analytes. GALDI is very sensitive for detecting those fatty

(50) Schwartz, S. A.; Reyzer, M. L.; Caprioli, R. M. *J. Mass Spectrom.* **2003**, *38*, 699−708.
(51) Claudio, G. A., P.; Simopoulos, E. T. *Effects of fatty acids and lipids in health and disease;* Karger: Basel, 1994.
(52) Halket, J. M.; Zaikin, V. G. *Eur. J. Mass Spectrom.* **2004**, *10*, 1−19.
(53) Nagy, K.; Jakab, A.; Fekete, J.; Vekey, K. *Anal. Chem.* **2004**, *76*, 1935−1941.
(54) Yang, W. C.; Adamec, J.; Regnier, F. E. *Anal. Chem.* **2007**, *79*, 5150−5157.

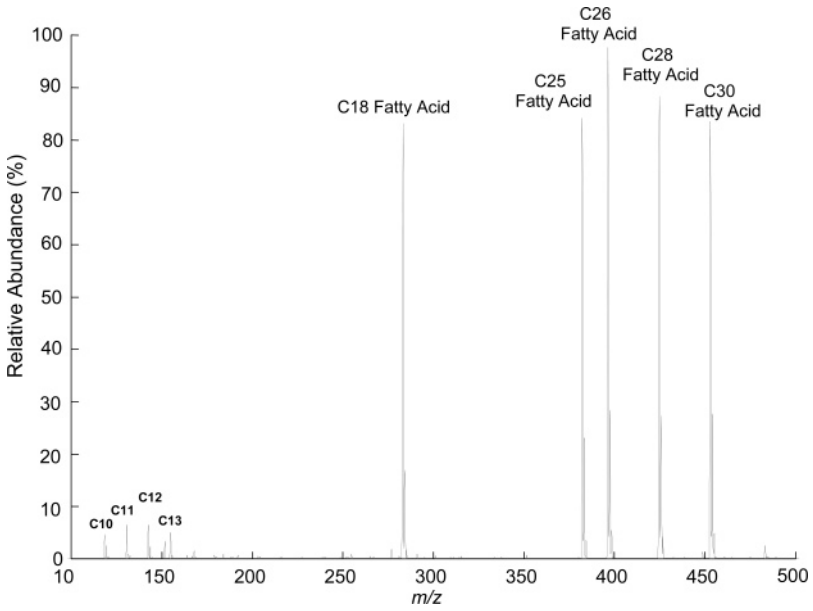

Figure 1. Mass spectrum of fatty acid standards (C18−C30 fatty acids) with GALDI in the negative-ion mode. Sample loading, 200 pmol of each.

acids in the negative-ion mode. Figure S1 in Supporting Information shows the spectrum of the fatty acid mixture with sample loading of 100 fmol of each on a 3-mm-diameter spot. Such fatty acids can also be detected as potassium adduct ions ($[M + K]^+$) in the positive-ion mode (data not shown), although the detection sensitivity (detection limit: 50 pmol/spot) is not as good as in the negative-ion mode.

Another group of standards tested were natural phenolic molecules, the flavonoids. It was estimated that 2% of all carbon photosynthesized by plants is converted into flavonoids or related compounds.[55] They have been reported to have antioxidant, antiatherosclerotic, and antineurodegenerative properties and are also known to be beneficial for the prevention of chronic diseases like cancer and heart diseases.[56,57] In the positive-ion mode, quercetin, kaempferol, and apigenin were detected as $[M + H]^+$ in both MALDI and GALDI experiments (Figure S2a−c in Supporting Information). $[M + Na]^+$ and $[M + 2Na - H]^+$ions for these three flavonoids can also be detected with GALDI. Phloretin was not detected with any of the three matrixes. This suggests that the center ring in the other three flavonoids plays an important role for protonation. However, it was possible to detect phloretin with GALDI in the negative-ion mode (Figure S2f). Several peaks in the region of m/z 150−200 in the spectra were identified as in-source fragments for the flavonoids by using tandem MS. For example, m/z 167 was identified as a fragment of phloretin while m/z 151 and 179 were fragments of quercetin. Unlike GALDI, which has a clean background, with DHB and CHCA, matrix peaks are predominant and none of the four flavonoid standards were detected in the negative-ion mode (Figure S2d,e). With GALDI, the negative-ion mode provides better sensitivity for detection of those flavonoid standards than the positive-ion mode does. The detection limits are 50 and 200 fmol/3-mm-diameter spot, respectively.

The third group of standards selected were oligosaccharides. Due to the lack of acidic or basic groups, they are difficult to be ionized with conventional MALDI. DHB can be used to detect large oligosaccharides (>1000 Da),[58] but smaller oligosaccharides are strongly interfered with by matrix ions. We tested oligosaccharides between 150 and 700 Da with DHB (Figure S3a), CHCA (Figure S3b), and graphite matrixes (Figure 2). With CHCA, only larger molecules like LacNAc, maltotriose, and maltotetraose can be detected as $[M + Na]^+$ but not the smaller ones such as ribose, glucose, and sucrose. DHB works slightly better than CHCA in that the small oligosaccharides such as glucose and sucrose can be detected. However, the intensities of the small saccharide peaks were very low. For example, [ribose + $Na]^+$ and [glucose + $Na]^+$ peaks are strongly suppressed as they are very close to matrix peaks $[DHB + Na]^+$ and $[DHB + 2Na - H]^+$, respectively. LacNAc has the highest detection sensitivity among all the oligosaccharides. This may suggest that the *N*-acetyl group has more affinity for sodium ions than the other moieties of oligosaccharides. In both the CHCA and DHB MALDI mass spectra (Figure S3a,b), the matrix peaks were predominant and oligosaccharides peaks were strongly interfered with. With GALDI, all six oligosaccharides were detected as $[M + Na]^+$ with decent signal-to-noise ratios, as shown in Figure 2. $[M + Na - 18]^+$ peaks were also observed for all five oligosaccharides as water loss (Figure 2). Neutral loss (NL) of 60 is known to result from the major cross-ring cleavage fragments of oligosaccharides with 1,4 linkages.[59] Here, m/z 629 and 467 were observed as such fragments of maltotetraose and maltotriose, respectively. The peak at m/z 305 corresponds to the major fragment of LacNAc. All of the above fragments were verified by tandem MS (data not shown). All cross-ring cleavage fragments are marked with asterisks in Figure 2. That the positive-ion mode of GALDI gave a noisier background compared to the negative-ion mode did not prevent the successful detection of small oligosaccharides. Small

(55) Robards, K.; Antolovich, M. *Analyst* **1997**, *122*, R11−R34.
(56) Seeram, N. P.; Lee, R.; Scheuller, H. S.; Heber, D. *Food Chem.* **2006**, *97*, 1−11.
(57) Törrönen, R. a. M., K. *Acta Hortic. (ISHS)* **2002**, 797−803.
(58) Harvey, D. J.; Martin, R. L.; Jackson, K. A.; Sutton, C. W. *Rapid Commun. Mass Spectrom.* **2004**, *18*, 2997−3007.
(59) Asam, M. R.; Glish, G. L. *J. Am. Soc. Mass Spectrom.* **1997**, *8*, 987−995.

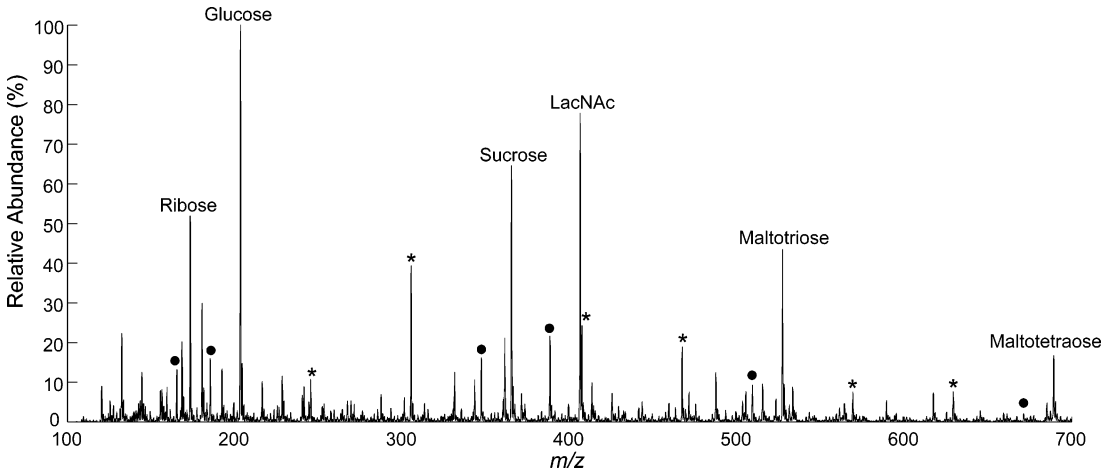

Figure 2. Mass spectrum of oligosaccharide standards with GALDI in the positive-ion mode. Sample loading, 100 ng of each. Peaks with ●, water loss fragments; peaks with *, major ring-cleavage fragments.

Table 1. List of Compounds Detected Directly from Apple and Strawberry and Their Average Concentrations (from the Literature)[a]

apple			strawberry		
m/z	peaks assigned	concns, g/kg	*m/z*	peaks assigned	concn, g/kg
		Organic Acids			
133[M−H]$^-$	malic acid	4.9×10^{-3} [60]	175 [M−H]$^-$	ascorbic acid*	0.59
191 [M−H]$^-$	quinic acid	0.76×10^{-3} [60]	191 [M−H]$^-$	citric acid	6.9−12.6 [62]
255 [M−H]$^-$	palmitic acid	0.24	255 [M−H]$^-$	palmitic acid	0.12
277 [M−H]$^-$	linolenic acid	0.09	277 [M−H]$^-$	linolenic acid	0.65
279 [M−H]$^-$	linoleic acid	0.43	279 [M−H]$^-$	linoleic acid	0.90
281 [M−H]$^-$	oleic acid	0.07	281 [M−H]$^-$	oleic acid	0.42
		Phenolics			
273 [M−H]$^-$	phloretin	4.7×10^{-3} [60]	269 [M−H]$^-$	apigenin	0.00−0.01
289 [M−H]$^-$	epicatechin	47.1×10^{-3}	285 [M−H]$^-$	kaempferol	4.6×10^{-3}
301 [M−H]$^-$	quercetin	45.7×10^{-3}	301[[M−H]$^-$	ellagic acid	0.06−0.5 [63]
435 [M−H]$^-$	phloridzin*	55.9×10^{-3} [61]	301[M−H]$^-$	quercetin	11.4×10^{-3}
447 [M−H]$^-$	quercetin glucosides*	0.13 [61]	431[M−H]$^-$	apigenin glucosides*	
		Oligosaccharides			
179 [M−H]$^-$	glucose/	83.3	179 [M−H]$^-$	glucose/	44.3
203 [M+Na]$^+$	fructose*		203 [M+Na]$^+$	fructose*	
219 [M+K]$^+$			219 [M+K]$^+$		
341 [M−H]$^-$	sucrose	20.7	341 [M−H]$^-$	sucrose	4.7
365 [M+Na]$^+$			365 [M+Na]$^+$		
381 [M+K]$^+$			381 [M+K]$^+$		

[a] All species have been checked by *m/z* against standards, and all but those with marked with asterisks have been checked by tandem MS. Except as noted, all other concentration data come from (1) ref 64 and (2) ref 65.

oligosaccharides such as hexose (glucose or fructose) and sucrose can also be detected as [M − H]$^-$ under the negative-ion mode peaks, vide infra. The detection sensitivity of oligosaccharides with GALDI under positive-ion mode is better than with GALDI under negative-ion mode. For instance, the detection limit of sucrose is 20 and 100 pmol/3-mm-diameter spot, respectively. This can be understood as oligosaccharides have neither carboxyl groups as fatty acids nor aromatic rings as flavonoids that can stabilize the deprotonated phenol group.

Direct Detection of Small Metabolite Molecules from Fruit Samples. Because of the sensitivity and background issues, GALDI in the positive-ion mode was used to detect oligosaccharides and the negative-ion mode was used to detect other metabolite molecules from fruit samples. Unlike experiments with the standards, colloidal graphite solution was applied on top of the sample; otherwise, the graphite particles may not be accessed by laser irradiation. For imaging purposes, homogeneous coverage over the sample area is a must. The application methodology has been optimized for IMS of mouse brain tissues in our previous work[38] and was used in this study without modification.

A list of small molecules detected directly from apple and strawberry samples was summarized in Table 1, with concentration data wherever available.[60−65] All identifications were made by comparing the MS spectra with those of standards. MS/MS data

(60) Gokmen, V.; Artik, N.; Acar, J.; Kahraman, N.; Poyrazoglu, E. *Eur. Food Res. Technol.* **2001**, *213*, 194−199.
(61) Lee, K. W.; Kim, Y. J.; Kim, D. O.; Lee, H. J.; Lee, C. Y. *J. Agric. Food Chem.* **2003**, *51*, 6516−6520.
(62) Skupien, K.; Oszmianski, J. *Eur. Food Res. Technol.* **2004**, *219*, 66−70.
(63) Williner, M. R.; Pirovani, M. E.; Guemes, D. R. *J. Sci. Food Agric.* **2003**, *83*, 842−845.

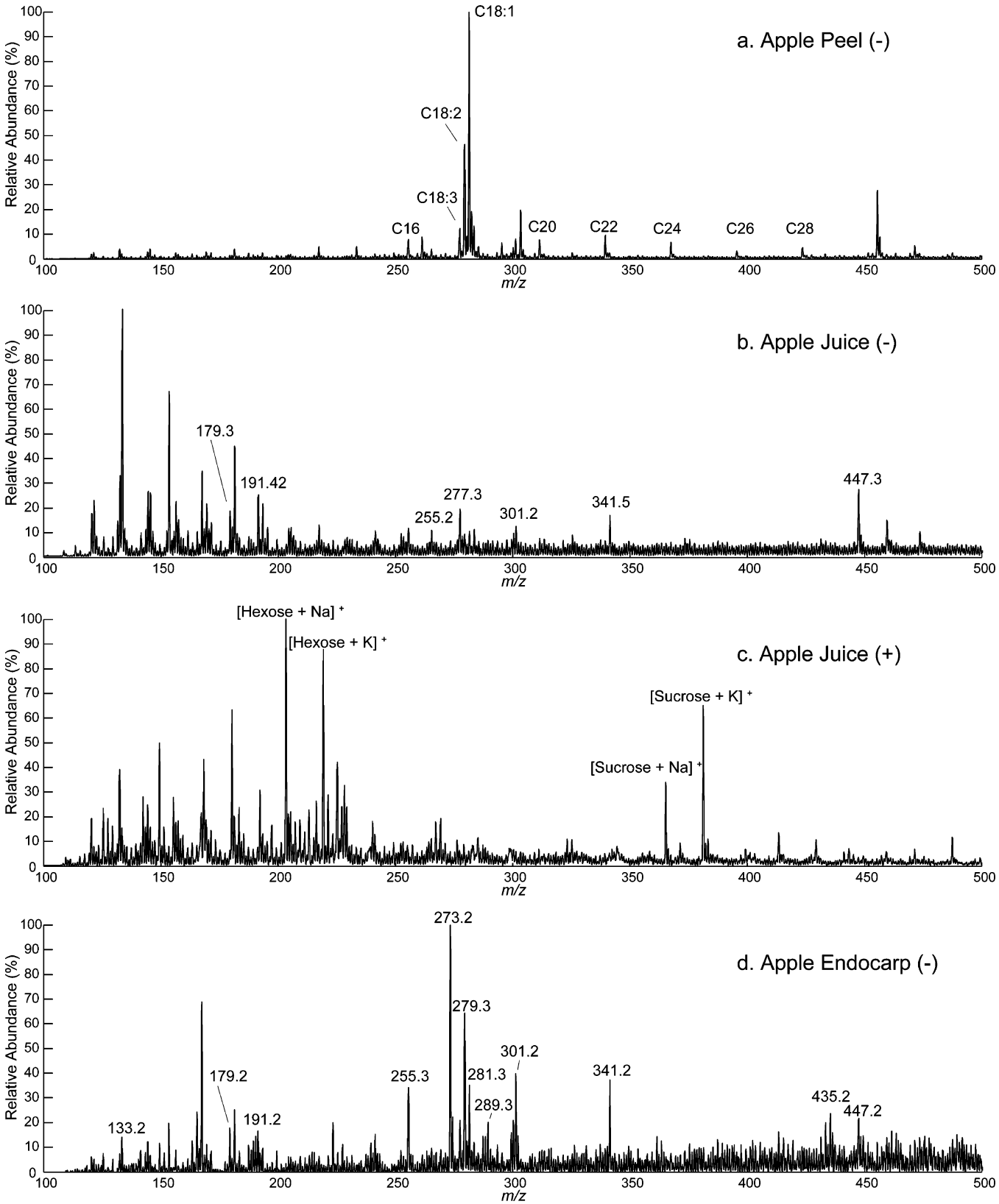

Figure 3. Representative GALDI mass spectra from different parts of apple. (a) Fatty acids composition on the outside of apple peel, negative-ion mode; (b) fresh apple juice, negative-ion mode; (c) hexose and sucrose from fresh apple juice, positive-ion mode; and (d) apple core, negative-ion mode. See Table 1 for peak identification in (b) and (d).

were also compared with those of standards except those at too low a concentration to give meaningful MS/MS data, as marked with asterisks. Tandem MS data are indispensable to identify isobaric ions, such as m/z 191, which were observed from both apple and strawberry. Tandem mass data of m/z 191 from apple and strawberry flesh are shown in Figure S4. Notably, citric acid

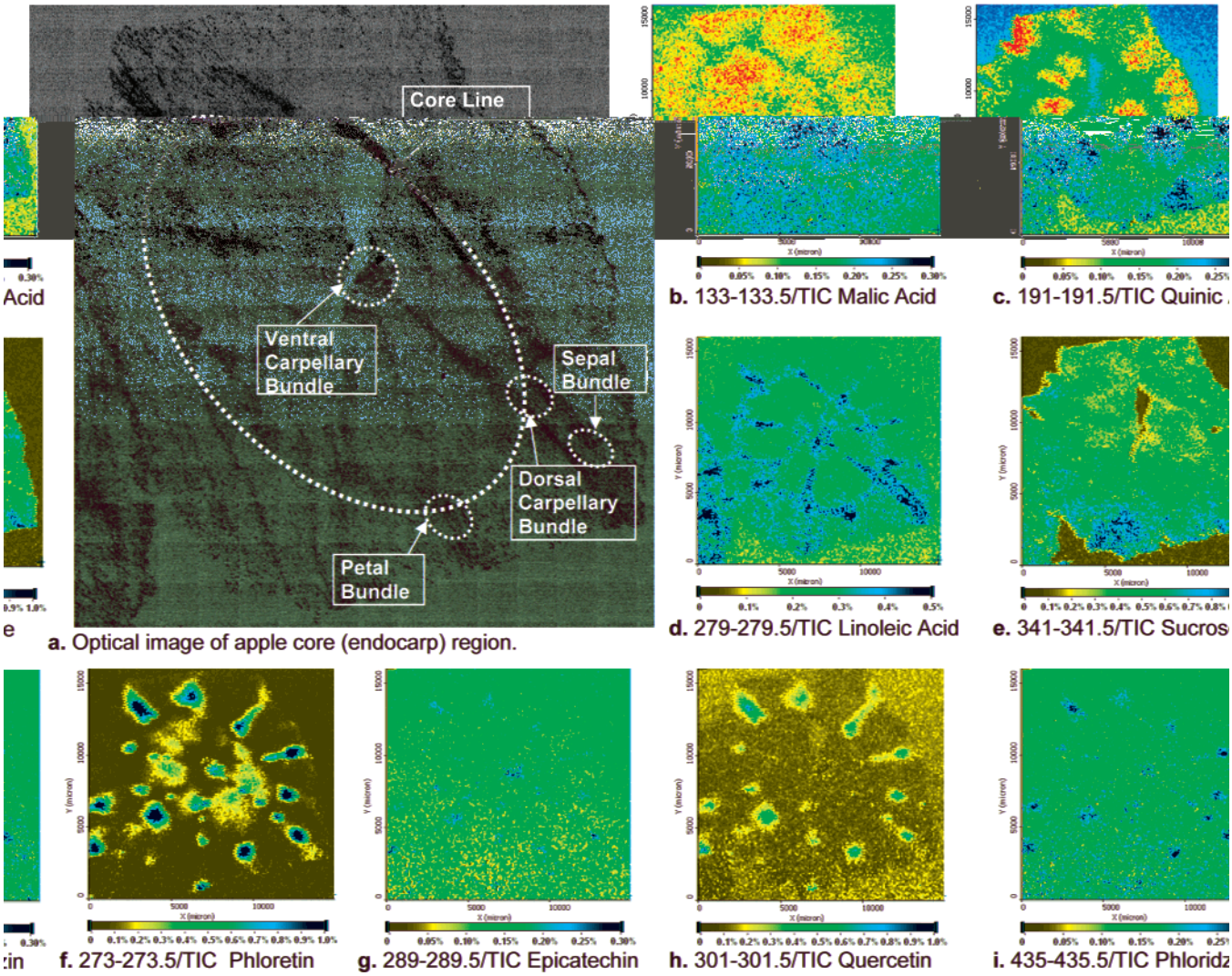

Figure 4. Chemically selective images of major ionic species identified from apple endocarp region with GALDI in the negative-ion mode. (a) Optical image taken with reversed color; (b) malic acid; (c) quinic acid; (d) linoleic acid; (e) sucrose; (f) phloretin; (g). epicatechin; (h) quercetin; and (i) phloridzin. All peak intensities were normalized by dividing by the total ion current (TIC) of each spectrum.

gave a predominant product ion at m/z 111 while quinic acid has specific product ions at m/z 85, 93, and 127, as reported previously.[66] By tandem MS it was confirmed that the peaks at m/z 191 were from quinic acid in apple while such peak came from citric acid in strawberry.

Figure 3 shows typical mass spectra taken from different parts of the apple. Fruits in supermarkets were always coated with a thin layer of wax for preservation and for better appearance. Fatty acids are one major class of components of wax and many of those up to C28 fatty acids were detected from apple peel, as shown in Figure 3a. Other compounds such as sugars or flavonoids were absent from the mass spectrum. The reason may be that such compounds were covered by the wax layer and were not accessible. Fatty acids may be naturally present on the apple peels as well; however, those cannot be discriminated from the species in the artificial wax layer.

As shown in Figure 3b, fresh apple juice gave malic acid, quinic acid, palmitic acid, and linolenic acid in the negative-ion mode. Hexose (glucose or fructose) and sucrose were detected as deprotonated ions as m/z 179 and 341, respectively. Quercetin is one of the major flavonoids contained in apple, and it was also detected. Figure 3c shows the spectrum in the positive-ion mode. Sodium adduct ions of hexose and sucrose were detected, as well as potassium adduct ions. According to the USDA nutrient database, fruits usually contain much higher amounts of potassium than sodium (90 vs 0 mg/100 g for apple and 292 mg vs 37 mg/100 g for strawberry).[64]

Figure 3d is the representative spectrum taken from the apple core (endocarp). Here, organic acids such as malic acid and quinic acid were still observed, but the relative intensities were not as high as those from juice. On the other hand, higher amounts of flavonoids such as phloretin and quercetin accumulated in the endocarp region. Apple peel also contains a lot of flavonoids, and quercetin was the predominant one found on the inside of apple peel (data not shown).

Figure S5a and b are representative mass spectra taken from strawberry. As reported previously with IR-MALDI,[49] strawberry

(64) See the USDA National Nutrient Database at: http://www.nal.usda.gov/fnic/foodcomp/search/, 2007.
(65) See the USDA National Nutrient Database at: http://www.nal.usda.gov/fnic/foodcomp/Data/Flav/flav.pdf, 2007.
(66) Ng, L. K.; Lafontaine, P.; Vanier, M. *J. Agric. Food Chem.* **2004**, *52*, 7251−7257.

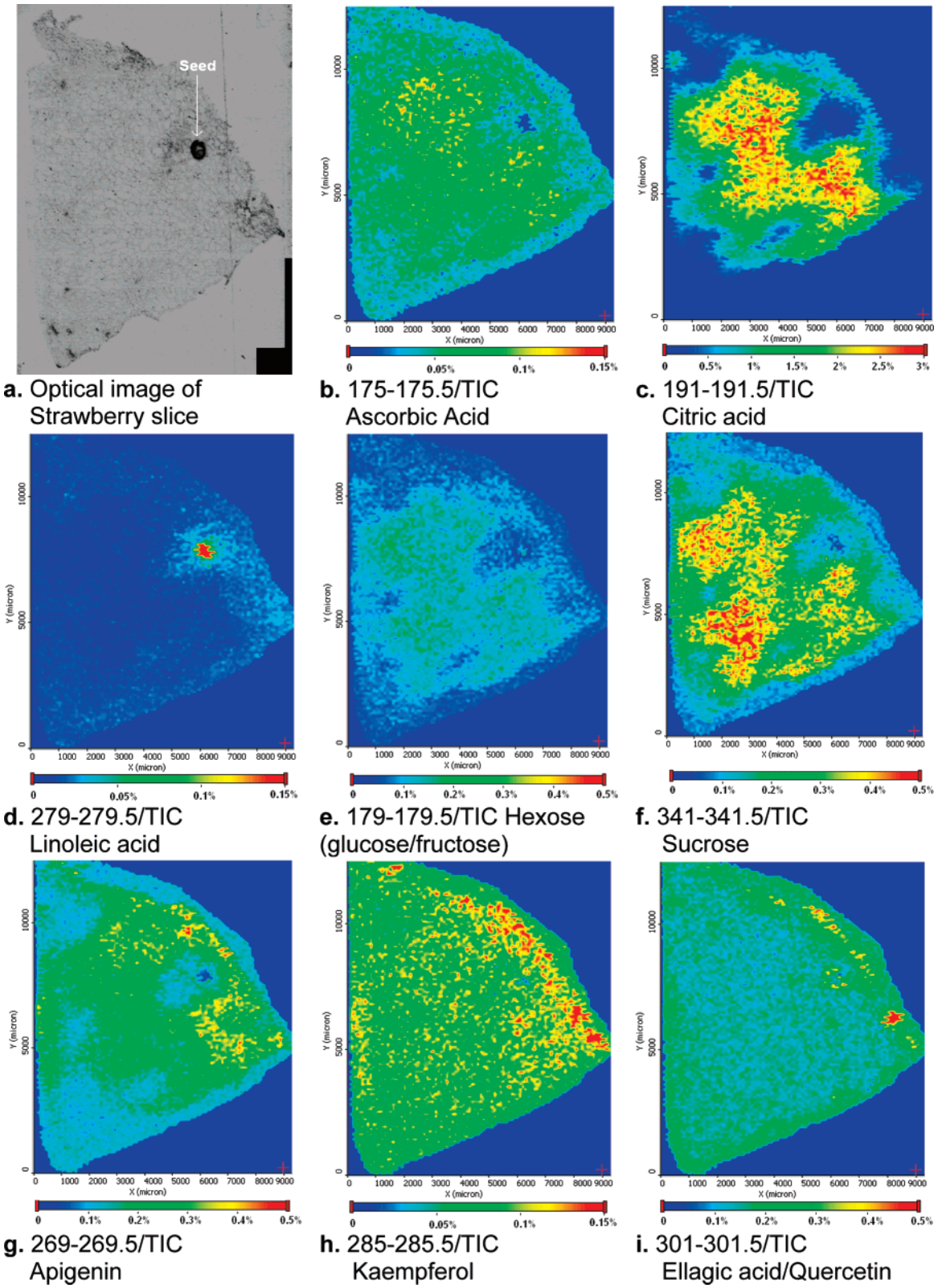

Figure 5. Chemically selective images of the major ionic species identified from strawberry with GALDI in the negative-ion mode. (a) Optical image taken with reversed color. One seed was present as the darkest dot on the right-hand side; (b) ascorbic acid; (c) citric acid; (d) linoleic acid; (e) hexose; (f) sucrose; (g) apigenin; (h) kaempferol; and (i) m/z 301−301.5 ellagic acid + quercetin. All peak intensities were normalized by dividing by the TIC of each spectrum.

contains a lot of citric acid. In our study, citric acid (m/z 191) was always the most intense peak in the negative-ion mode. GALDI can also detect those compounds that were too low in concentration to be detected by IR-MALDI, such as ascorbic acid and ellagic acid. Quercetin and kaempferol was also detected in the red part of strawberry (more details in IMS data below). Other

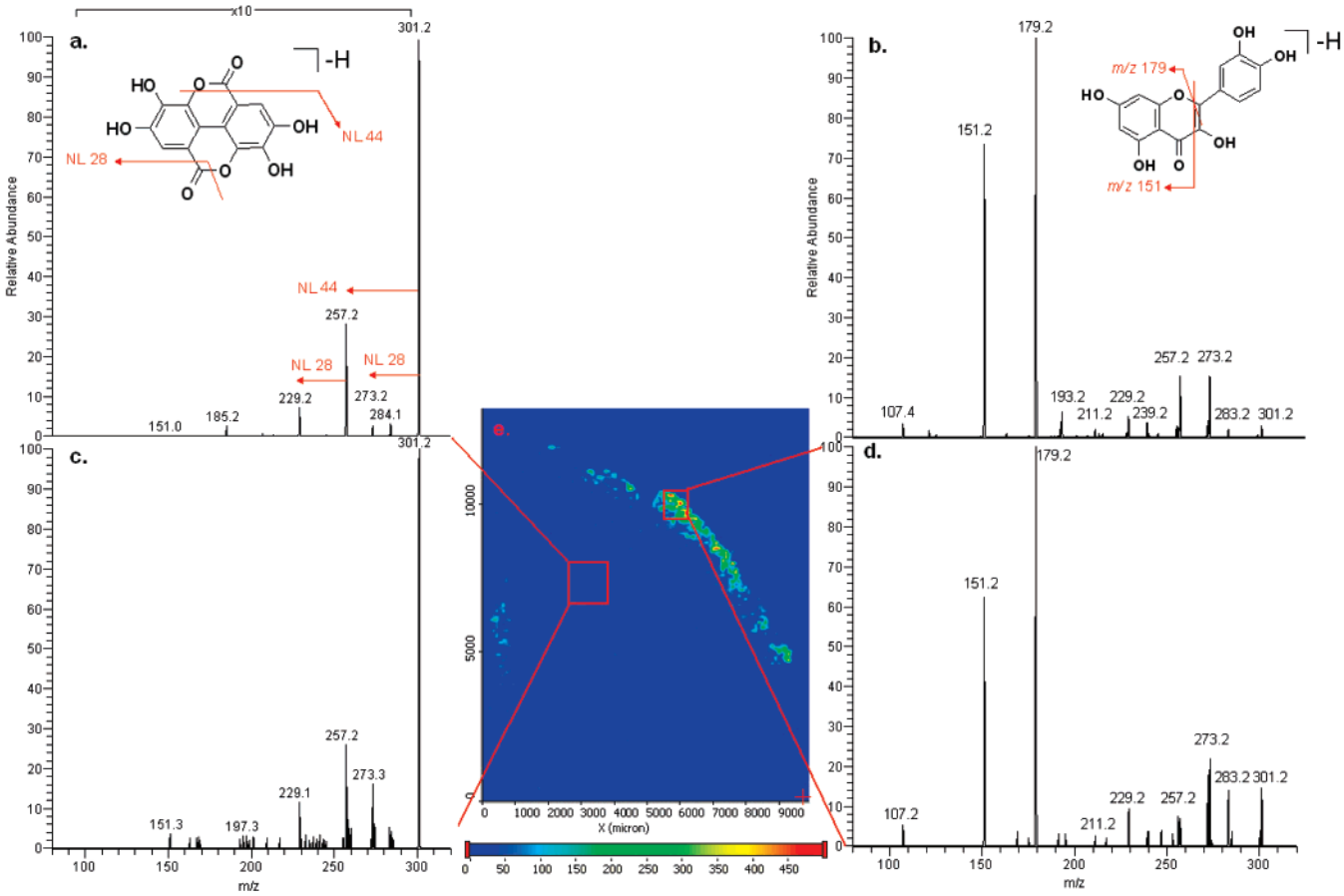

Figure 6. Product ion spectra of *m*/*z* 301 from (a) ellagic acid standard, (b) strawberry flesh, (c) quercetin standard, (d) edge of strawberry, and (e) chemically selective image for product ion at *m*/*z* 179 (precursor ion *m*/*z* 301) of strawberry slice with GALDI. All spectra were collected in the negative-ion mode. The proposed fragment pathways are shown as insets.[67]

deprotonated ions include palmitic acid, oleic acid, apigenin, hexose, and sucrose, as marked in Figure S5a. Similar to the previous report,[49] citric acid and sucrose were barely detected in the seed region, as shown in Figure S5b. Instead, C16 and unsaturated C18 fatty acids were the major components.

IMS of Metabolites from Apple and Strawberry. IMS in the negative-ion mode was performed to show the detailed distributions of different metabolite molecules on apple and strawberry slices, as Figure 4 and Figure 5, respectively. Small molecules such as malic acid, quinic acid, and sucrose distributed relatively evenly over the apple flesh part, as shown in Figure 4b, c, and e. Long-chain fatty acid such as linoleic acid was detected all over the slice, but more accumulated along the core line and bundles, as shown in Figure 4d. Flavonoids also accumulated more in the core region but not in the flesh, as shown in Figure 4f–i. Unlike linoleic acid, they seem to be only enriched in the bundles (both sepal and pedal), but not along the core line. Another interesting feature is that flavonoids were found in the ventral carpellary bundle (center of the apple slice) except for quercetin.

The images shown in Figure 5 were scanned from a pie-shaped strawberry slice, with the red skin on the right-hand side and one seed in the middle-right part. Citric acid, apigenin, hexose and sucrose were distributed all over the flesh, while fatty acids such as linolenic and linoleic acids accumulated on the seed. The peak at *m*/*z* 301.2 was detected all over the strawberry with a relatively constant concentration in the flesh, but showed higher local intensity on the outside (red part) and the seed areas. The candidates were quercetin (MW 302.24) and ellagic acid (MW 302.20), and the two species could be distinguished in tandem MS. Panels a and b in Figure 6 show the MS/MS spectra of ellagic acid and quercetin standards. *m*/*z* 151 and 179, were specific fragments of quercetin due to the cleavage of the center ring, as reported previously;[56,67] while ellagic acid is more rigid and only small fragments such as NL 28 and NL 44 were observed. MS/MS product ion spectra from strawberry flesh were similar to those from ellagic acid (Figure 6c), while those at *m*/*z* 301.2 on the edge gave quercetin-like fragments (Figure 6d). The chemically selective ion image at *m*/*z* 179 with precursor ions at *m*/*z* 301.2 is shown in Figure 6e. The ambiguity in Figure 5i is thus resolved.

Similarly, both citric acid (MW 192.13) and quinic acid (MW 192.17) were detected as *m*/*z* 191 with GALDI in the negative-ion mode. IMS/MS (data not shown) with precursor ions at *m*/*z* 191.2 showed that product ions at *m*/*z* 111.3 were detected all over the strawberry slice, while no specific fragments of quinic acid (*m*/*z* 85 or 93) were observed. This suggests that all *m*/*z* 191 ions from strawberry were from citric acid (Figure 5c).

(67) Chen, M. L.; Song, F. R.; Guo, M. Q.; Liu, Z. Q.; Liu, S. Y. *Rapid Commun. Mass Spectrom.* **2002**, *16*, 264–271.

ACKNOWLEDGMENT

E.S.Y. thanks the Robert Allen Wright Endowment for Excellence for support. The Ames Laboratory is operated for the U.S. Department of Energy by Iowa State University under Contract DE-AC02-07CH11358. This work was supported by the Director of Science, Office of Basic Energy Sciences, Divisions of Chemical Sciences and Biosciences.

SUPPORTING INFORMATION AVAILABLE

Detailed mass spectra of standards and fruit samples. This material is available free of charge via the Internet at http://pubs.acs.org.

Received for review March 28, 2007. Accepted June 25, 2007.

AC0706170